Atomistic Simulation of Dislocation-Defect Interactions in Cu

B. D. Wirth[a], V. V. Bulatov and T. Diaz de la Rubia, Chemistry and Materials Science Directorate, Lawrence Livermore National Laboratory, Livermore, CA 94550

OBJECTIVE

The mechanisms of dislocation-defect interactions are of practical importance for developing quantitative structure-property relationships, mechanistic understanding of plastic flow localization and predictive models of mechanical behavior in metals under irradiation. In copper and other face centered cubic metals, high-energy particle irradiation produces hardening and shear localization. Post-irradiation microstructural examination in Cu reveals that irradiation has produced a high number density of nanometer sized stacking fault tetrahedra. Thus, the resultant irradiation hardening and shear localization is commonly attributed to the interaction between stacking fault tetrahedra and mobile dislocations, although the mechanism of this interaction is unknown. In this work, we present a comprehensive molecular dynamics simulation study that characterizes the interaction and fate of moving dislocations with stacking fault tetrahedra in Cu using an EAM interatomic potential. This work is intended to produce atomistic input into dislocation dynamics simulations of plastic flow localization in irradiated materials.

SUMMARY

It is well established that irradiation of metals by high-energy neutrons and ions produces significant changes in material microstructure and mechanical properties [1-5]. In low stacking fault energy face centered cubic (fcc) metals, stacking fault tetrahedra (SFT) are the primary defect observed following high-energy particle irradiation. For example, post-irradiation microstructural examination of copper irradiated at temperatures between 20 and 100 °C and doses between 10^{-4} and 10^2 dpa reveals that approximately 90% of the high number density (about 10^{23} m^{-3}) of radiation-induced defects are SFTs and that the average SFT size remains constant at about 2.5 ± 0.5 nm [3,6]. When deformed after irradiation, Cu and other low stacking fault energy fcc metals exhibit significant mechanical property degradation, including a sharp increase in yield stress, a decrease in ductility and often, plastic flow localization in the form of defect-free dislocation channels [2,5]. The formation of dislocation channels is commonly attributed to dislocation absorption of the vacancies contained in SFTs [7]. However, a concise atomistic picture of the SFT absorption mechanism is lacking. Thus, the objective of this work is to obtain atomistic insight into the interaction of SFTs with dislocations, necessary to understand radiation-induced mechanical property changes.

[a] Corresponding author contact information: phone (925) 424-9822, fax (925) 423-7040, wirth4@llnl.gov

Computer simulation studies have been used to successfully model the production and accumulation of damage in irradiated Cu [8-13] and some key results of our work are briefly summarized here. Molecular dynamics (MD) simulations of displacement cascade evolution in Cu reveal the formation of large vacancy and self-interstitial loops [8-10]. The self-interstitial cluster loops undergo easy, one-dimensional transport [11] and are assumed to rapidly migrate away from the vacancy rich cascade region. The clustered vacancies then collapse to form SFTs, which occurs within a few picoseconds at room temperature by a dislocation mechanism[12], consistent with that first proposed by Silcox and Hirsch [14]. Interestingly, a number of MD simulations predict that the SFT structure will not consist of perfect tetrahedron, but in most cases, will actually consist of truncated tetrahedron [12,15] and in some cases, overlapping, truncated SFTs[1] [12].

SIMULATION METHODOLOGY

MD simulations of the interaction and fate of moving edge dislocations in Cu were performed using the MDCASK code [16] and an embedded atom method (EAM) potential [17,18]. The elastic constants and stacking fault energy obtained with the EAM potential are provided in Table 1. The simulations were performed in a cubic cell bounded by <111>, <110> and <112> faces, as sketched in Figure 1. Periodic boundary conditions are applied in the Y=[110] and Z=[1$\bar{1}$2] directions, while the X=[$\bar{1}$11] faces are free surfaces. An edge dislocation is introduced in the simulation cell by removing two (220) half-planes and equilibrating the system at 100 K to allow the edge dislocation, **b**=a/2<110>{111}, to split into two Shockley partial dislocations, **b**=a/6<112>{111}, separated by a stacking fault. SFT and overlapping, truncated SFTs were also inserted into the simulation cell on the ($\bar{1}$11) glide plane ahead of the dissociated edge

Table 1 – Elastic constants and stacking fault energy obtained from the EAM Cu potential [17,18] used in this work.

C_{11}	176 GPa
C_{12}	129 GPa
C_{44}	82.3 GPa
μ	58.8 GPa
Stacking fault energy	11.4 mJ/m^2

---

[1] A triangular vacancy platelet on a {111} plane bounded by three <110> directions forms a single SFT. A triangular vacancy platelet bounded by two <110> and one <112> directions forms two partial (truncated) SFTs, one above and one below the initial plane; we define this as an overlapping truncated SFT.
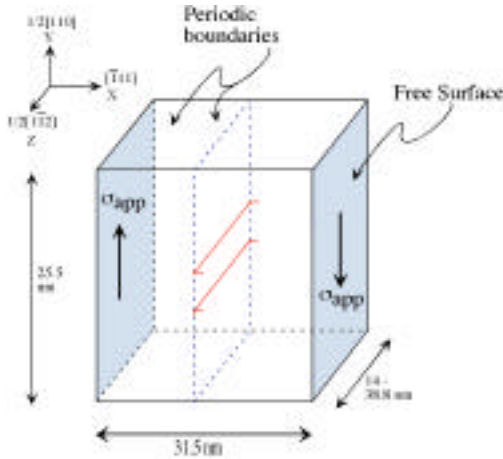
Figure 1 = Schematic view of the simulation cell and dimensions used in this work.

dislocation. Following equilibration at 100 K, a constant shear stress, $_{yx}$, is applied by superimposing a constant force in the [110] direction on the atoms in the two ($\bar{1}1l$) surfaces.

In the results reported here, the simulation cell was 31.2 nm in X, 25.5 nm in Y and either 14.0 or 38.8 nm in Z (along the dislocation line), corresponding to a dislocation density of about 8×10^{14} m^{-2} and a SFT density of 3 to 9×10^{22} m^{-3}. The dislocation and SFT are visualized by plotting the location of atoms with high potential energy.

RESULTS AND DISCUSSION

Figure 2 shows a series of MD simulation snapshots of the ($\bar{1}1l$) glide plane (in [$\bar{1}11$] projection) of the interaction between a moving, dissociated edge dislocation and a SFT which lies across the dislocation glide plane. The simulation was performed at an initial temperature of 100 K and an applied shear stress of 300 MPa. It is important to mention some additional details regarding this simulation. First, as shown in Table 1, the Cu EAM potential gives a stacking fault energy which is lower than experimental values (30-40 mJ/m^2) and results in a large equilibrium separation (~7-8 nm) between the two Shockley partials. Second, the applied stress is significantly higher than the yield stress of copper and is used to study the fate of the interaction within readily accessible MD simulation times. Additional simulations are ongoing to characterize the effect of these (and other) variables on the results.

Figure 2a shows the initial configuration of the edge dislocation, which is split into the two Shockley partial dislocations, and the SFT, which consists of 6 stair-rod dislocations when viewed using high potential energy atoms. Although not seen in this projection, the SFT overlaps the glide plane of the edge dislocation. Following application of the shear stress, the two Shockley partial dislocations are driven towards

the SFT. Figure 2b shows the position of the partial dislocations 9 ps after applying the 300 MPa shear stress. By this time, the leading Shockley partial dislocation has reached the SFT, felt a repulsive force and bowed back away from the SFT. As the trailing partial approaches, the leading partial is forced to enter the SFT (Figure 2c). The SFT acts as a hard barrier to dislocation motion and in order for the leading partial to move past the SFT, it must noticeably bow around it, finally releasing at a critical angle of about 80° (Figure 2d). By 15.5 ps (Figure 2e) the trailing partial enters the SFT, as the leading partial continues to move ahead with significant remaining curvature along its line. Interestingly, the SFT provides less resistance to the passage of the trailing partial and the shape of the trailing partial shows only a slight perturbation immediately after passing the SFT (Figure 2f).

Surprisingly, the SFT is not absorbed by the moving edge dislocation, but instead acts as a hard obstacle to dislocation motion. Following passage of the dislocation, the SFT has been sheared along the dislocation glide plane, and thus has a surface step (ledge) along three of its four {111} faces, but remains largely intact. Qualitatively similar results are observed in simulations of the edge dislocation – SFT interaction performed with a range of applied stress from 50 to 300 MPa, different SFT separation along the dislocation line and slightly different interaction geometry. In all cases, the SFT acts as a hard barrier and despite the formation of surface steps, remains intact following dislocation passage.

However, dislocation absorption of an SFT-type defect has been observed in the case where the SFT is not perfect, but rather consists of overlapping, truncated SFTs. Figure 3 shows the results of one such simulation at 100 K in Cu. In this simulation, an overlapping, truncated SFT such as formed by aging displacement cascades [12], with a spacing of 14 nm (along the dislocation line), is placed on the glide plane of a dissociated edge dislocation which moves under an applied shear stress of 300 MPa. Figure 3a shows the initial configuration of the edge dislocation, split into two Shockley partial dislocations, and the overlapping, truncated SFT (most easily visualized in <110> projection), as represented through visualization of the atoms with high potential energy. Figure 3b shows that upon contact, the leading partial absorbs vacancies from part of the overlapping truncated SFT and climbs, forming a pair of superjogs that effectively pin the leading partial as the trailing partial approaches. Figure 3c shows that the trailing partial catches the leading partial at the location of the overlapping SFT and superjog pair, climbs through absorption of the remaining vacancies in the defect and constricts at the location of the superjogs. Following defect absorption, the dislocation continues to move (Fig. 3d), but with a decreased mobility associated with the superjogs.
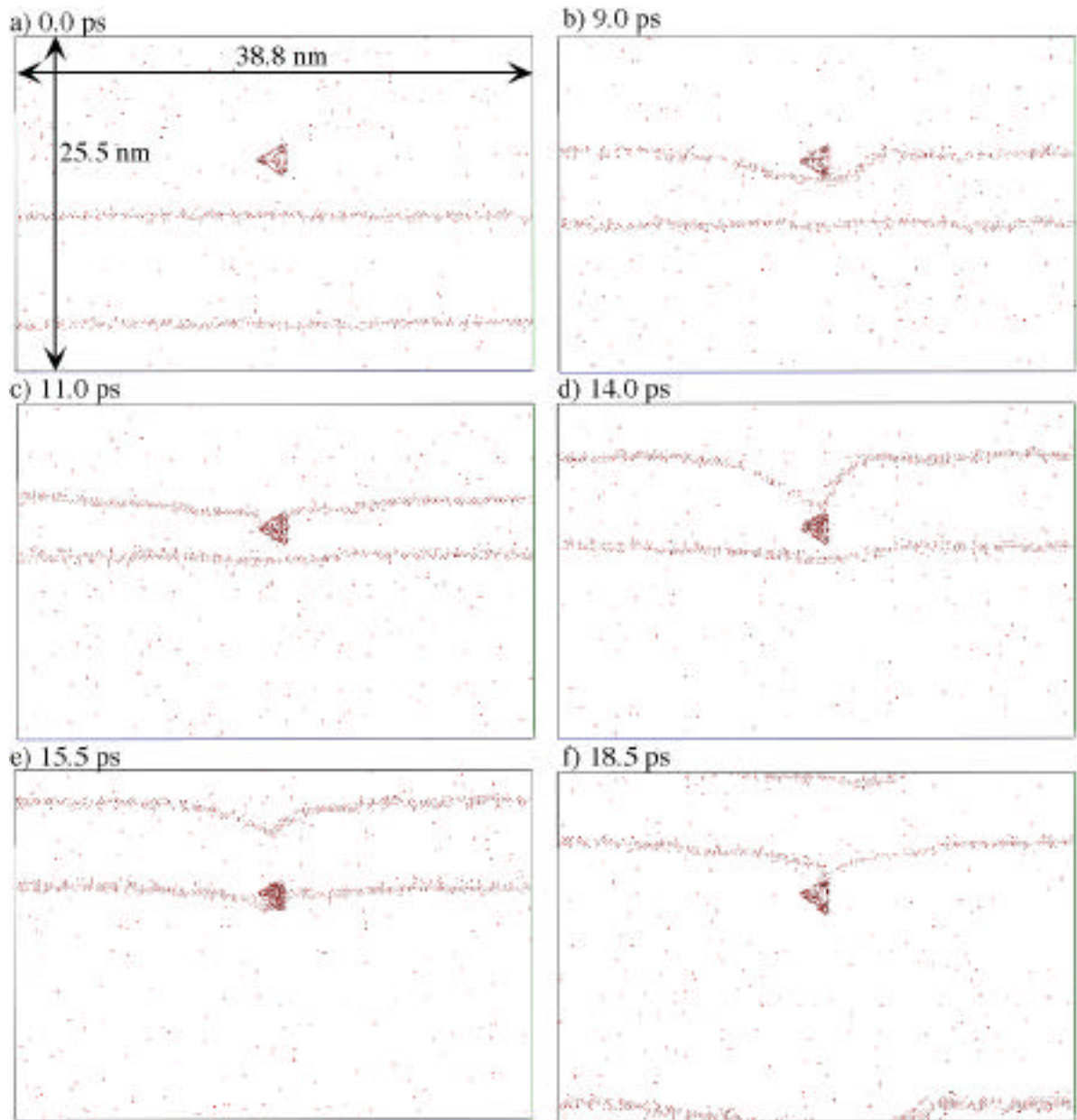
Figure 2 – [$\bar{1}$11] projection of MD simulation snapshots showing the interaction between a moving, dissociated edge dislocation and an SFT which overlaps the dislocation glide plane, as visualized by plotting atoms with high potential energy. Dislocation positions are shown at a) 0.0 ps, b) 9.0 ps, c) 11.0 ps, d) 14.0 ps, e) 15.5 ps and f) 18.5 ps after applying a 300 MPa shear stress. Note, the use of high potential energy atoms for visualization introduces thermal noise (isolated points) into the snapshots.
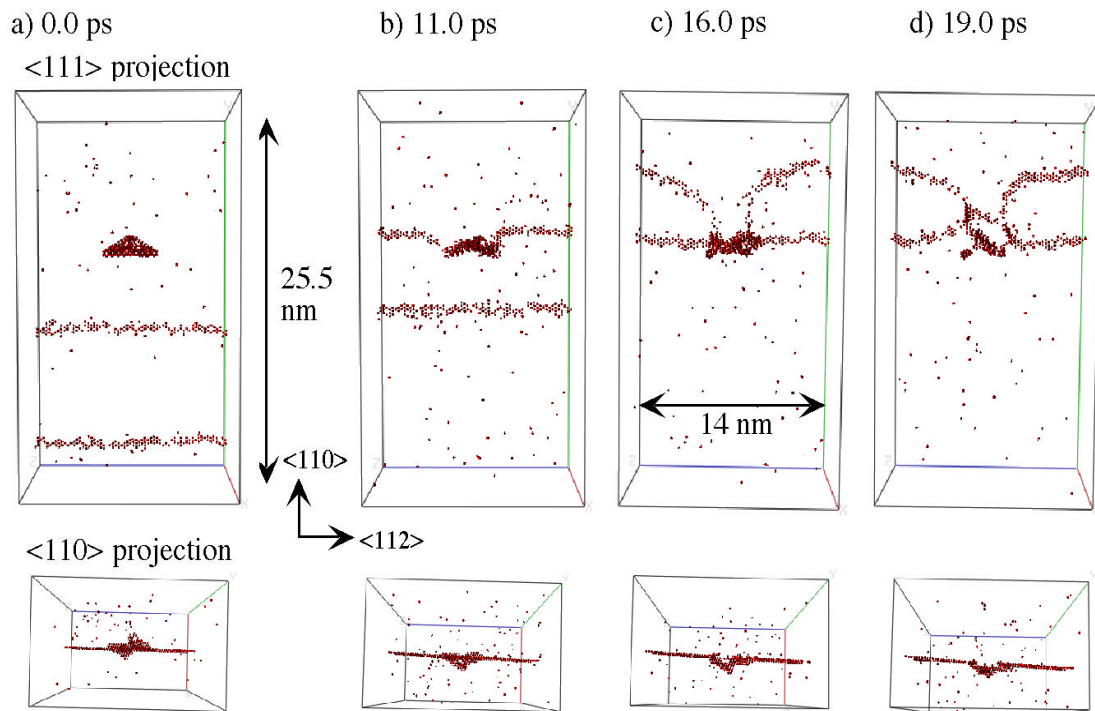
Figure 3 – MD simulation snapshots showing the interaction between a moving, dissociated edge dislocation and an overlapping, truncated SFT in Cu. The high potential energy atoms are visualized in <111> (top) and <110> (bottom) projections and show the motion of the two Shockley partials and interaction with the overlapping, truncated SFT at a) 0, b) 11.0, c) 16.0 and d) 19.0 ps after application of a 300 MPa shear stress. See text for additional details.

The detailed absorption mechanism is complicated and has not yet been completely analyzed. It is clear that passage of a single dislocation through a perfect SFT will not lead to its absorption, but it is not yet known how many dislocations are required to completely shear a SFT, or what degree of SFT truncation will result in absorption. However, it is clear that defect absorption produces dislocation climb and the formation of superjog pairs, which have decreased mobility. One of the superjogs is initially constricted, presumably in the form of a Lomer segment, as discussed by Rodney and Martin for the case of dislocation climb associated with self-interstitial cluster absorption [19]. The constricted superjog is essentially sessile, but can transform to a more favorable (glissile) configuration through the incorporation of three self-interstitials, as discussed in Ref. 19. This process occurred just prior to the snapshot shown in Fig. 3c, and indeed, the small cluster of high energy atoms seen below the left superjog in Fig. 3d has been identified to consist of three vacancies.

CONCLUSIONS

Selected results from a MD simulation study of the interaction between a moving edge dislocation and stacking fault tetrahedra defects have been presented. The results show that a perfect SFT acts as a hard obstacle for dislocation motion and, although the SFT is sheared by the dislocation passage, it remains largely intact. However, our simulations show that an overlapping, truncated SFT is absorbed by the passage of an edge dislocation, resulting in dislocation climb and the formation of a pair of less mobile super-jogs on the dislocation. Additional simulations are underway to characterize the matrix of possible dislocation-SFT interactions, including the effect of applied stress and stacking fault energy, and provide rules for dislocation dynamics simulations that can provide insight into the mechanisms responsible for flow localization in irradiated metals.

REFERENCES

1. L. K. Mansur and E. E. Bloom, *J. of Metals*, **34** (1982) 23.
2. G. E. Lucas, *J. Nuc. Mat* . **206** (1993) 287.
3. B. N. Singh and S. J. Zinkle, *J. Nuc. Mat..* **206** (1993) 212.
4. H. Trinkaus, B. N. Singh and A. J. E. Foreman, *J. Nuc. Mat.* **251** (1997) 172.
5. M. Victoria, N. Baluc, C. Bailat, Y. Dai, M. I. Luppo, R. Schaublin and B. N. Singh, *J. Nuc. Mat*. **276** (2000) 114.
6. Y. Dai, M. Victoria, Mat. Res. Soc. Symp. Proc., **439** (1997) 319.
7. N.M. Ghoniem, S.-S. Tong and L.Z. Sun, *Phys. Rev. B,* **139(1)** (2000) 913.
8. T. Diaz de la Rubia and M. W. Guinan, *Phys. Rev. Lett.* **66** (1992) 655.
9. W. J. Phythian, R. E. Stoller, A. J. E. Foreman, A. F. Calder and D. J. Bacon, *J. Nucl. Mat.* **223** (1995) 245.
10. R. S. Averback and T. Diaz de la Rubia, Solid State Physics, **51** (1998) 281.
11. Y. N. Osetsky, D. J. Bacon, A. Serra, B. N. Singh, and S. I. Y. Golubov, *J. Nucl. Mat.* **276** (2000) 65.
12. B. D. Wirth, V. Bulatov and T. Diaz de la Rubia, J. Nuc. Mat. (2000) in press.
13. M. J. Caturla, N. Soneda, E. A. Alonso, B. D. Wirth and T. Diaz de la Rubia, *J. Nuc. Mat.* **276** (2000) 13.
14. J. Silcox and P. B. Hirsch, *Phil. Mag.*, **4** (1959) 72.
15. Y. N. Osetsky and D. J. Bacon, this conference proceedings.
16. T. Diaz de la Rubia and M. W. Guinan, *J. Nuc. Mat.*, **174** (1990) 151.
17. S. M. Foiles, M. I. Baskes and M. S. Daw, *Phys. Rev. B*, **33** (1986) 7983.
18. M. Ghaly and R. S. Averback, personal communication.
19. D. Rodney and G. Martin, *Phys. Rev. B* **61** (2000) 8714.